JOURNAL OF BACTERIOLOGY, Aug. 2009, p. 5169–5179 Vol. 191, No. 16
0021-9193/09/$08.00+0 doi:10.1128/JB.00458-09

Role of Periplasmic Chaperones and BamA (YaeT/Omp85) in Folding and Secretion of Intimin from Enteropathogenic *Escherichia coli* Strains[▽]†

Gustavo Bodelón, Elvira Marín, and Luis Ángel Fernández*

Department of Microbial Biotechnology, Centro Nacional de Biotecnología, Consejo Superior de Investigaciones Científicas, Campus de Cantoblanco, 28049 Madrid, Spain

Received 3 April 2009/Accepted 3 June 2009

Intimin is a bacterial adhesin located on the surface of enteropathogenic *Escherichia coli* and other related bacteria that is believed to self-translocate across the outer membrane (OM), and therefore it has been regarded as a member of the type V secretion system (T5SS), which includes classical autotransporters (ATs). However, intimin has few structural similarities to classical ATs and an opposite topology with an OM-embedded N region and a secreted C region. Since the actual secretion mechanism of intimin is unknown, we investigated intimin biogenesis by analyzing its requirement of periplasmic chaperones (DsbA, SurA, Skp, and DegP) and of OM protein BamA (YaeT/Omp85) for folding, OM insertion, and translocation. Using full-length and truncated intimin polypeptides, we demonstrate that DsbA catalyzes the formation of a disulfide bond in the D3 lectin-like domain of intimin in the periplasm, indicating that this secreted C-terminal domain is at least partially folded prior to its translocation across the OM. We also show that SurA chaperone plays the major role for periplasmic transport and folding of the N region of intimin, whereas the parallel pathway made by Skp and DegP chaperones plays a secondary role in this process. Further, we demonstrate that BamA is essential for the insertion of the N region of intimin in the OM and that the protease activity of DegP participates in the degradation of misfolded intimin. The significance of these findings for a BamA-dependent secretion mechanism of intimin is discussed in the context of T5SSs.

Enteropathogenic and enterohemorrhagic *Escherichia coli* (EPEC and EHEC, respectively) strains are important pathogens causing severe diarrheal diseases and other acute symptoms (e.g., hemorrhagic colitis and hemolytic-uremic syndrome) (31). EPEC and EHEC bacteria adhere to the intestinal enterocytes, inducing a destruction of microvilli called attaching and effacing (A/E) lesions, which involves a strong rearrangement of host cell cytoskeleton and the formation of an actin "pedestal" beneath the adherent bacteria. The formation of A/E lesions requires an intimate attachment of the bacterium to the host cell membrane mediated by the interaction of a specific bacterial adhesin, intimin (*eaeA*), with its receptor in the host cell membrane, Tir (for translocated intimin receptor), which is translocated by the bacterium using a type III secretion system (19). Most genes required for A/E lesion formation (i.e., *eaeA*, *tir*, and those encoding the type III secretion system) are clustered in a pathogenicity island referred to as the locus of enterocyte effacement (LEE) (16). The LEE is also found in the genome of other intestinal pathogens that induce similar A/E lesions, such as *Citrobacter rodentium* (13).

Intimins are large polypeptides (ca. 95 kDa) displayed at the surfaces of LEE$^+$ pathogenic bacteria that contain distinct structural and functional N and C regions (Fig. 1A) (26). The N region of intimins (residues 1 to 550) anchors the protein in the bacterial envelope and is highly conserved among intimins from different strains (>95% identity). This region is predicted to have a long N-terminal signal peptide (residues 1 to 39) for Sec-dependent secretion across the inner membrane, followed by a short periplasmic LysM-type domain (residues 64 to 113), which could tether intimin to the peptidoglycan layer (8), and a large β-domain (residues 160 to 550) embedded in the outer membrane (OM) and predicted to fold as a β-barrel. The C region of intimins (residues 551 to 939, referred to as intimin α from EPEC strain E2348/69), is less conserved (ca. 50 to 70% identity) and forms a surface-exposed rigid rod that binds to Tir (17). This region comprises three immunoglobulinlike domains (named D0, D1, and D2) and a C-type lectinlike domain (D3) that directly interacts with Tir (3, 35). Interestingly, intimins have structural and sequence similarity with invasins from enteropathogenic *Yersinia* strains, which bind to β_1-integrins in the host cell to promote bacterial invasion (22).

The molecular mechanism used by intimin for its secretion is poorly understood, but a self-translocation model has been proposed in which the β-barrel of the N region inserts in the OM, forming a hydrophilic protein-conducting channel used for translocation of the C region to the cell surface (52). This model is inspired on the self-translocation mechanism proposed for classical autotransporters (ATs), in which a β-barrel found in the C regions of ATs inserts into the OM, assisting the secretion of the N region (the passenger domain) (12). Assuming a common self-translocation mechanism for ATs and intimin and/or invasins, some authors have included these proteins in the type V secretion system (38). However, the self-translocation of ATs has been challenged because the crystal structures of two β-barrel domains did not reveal the presence of a protein-conducting channel large enough for translocation of folded (or partially folded) passenger domains

* Corresponding author. Mailing address: Centro Nacional de Biotecnología–CSIC, Campus de Cantoblanco, Madrid 28049, Spain. Phone: 34 91 585 48 54. Fax: 34 91 585 45 06. E-mail: lafdez@cnb.csic.es.

† Supplemental material for this article may be found at http://jb.asm.org/.

▽ Published ahead of print on 12 June 2009.

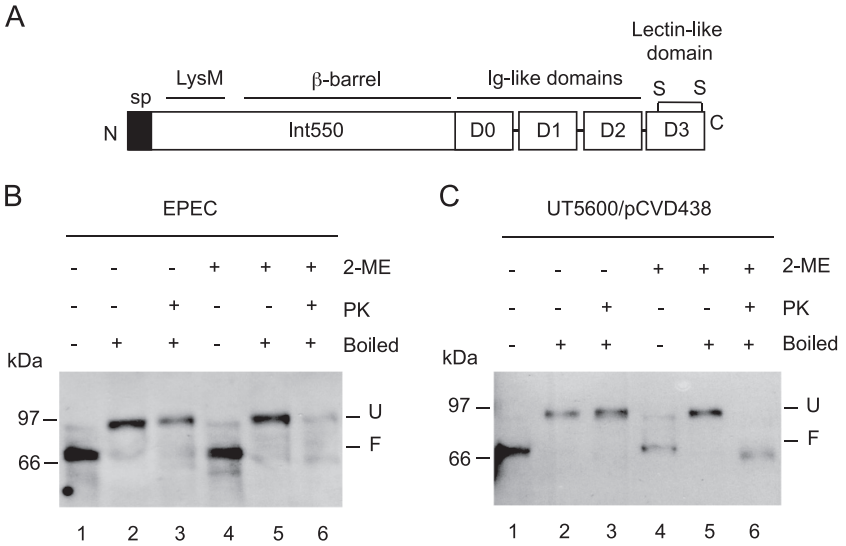

FIG. 1. Intimin domain organization and expression in EPEC and *E. coli* K-12. (A) Schematic drawing of intimin illustrating its domain organization. The first 550 amino acid residues of intimin (Int550) contain a signal peptide (sp) located at the N terminus (N), a putative peptidoglycan-binding domain (LysM), and an OM-embedded domain predicted to fold as a β-barrel. The immunoglobulinlike (D0, D1, and D2) and the lectinlike (D3) domains are displayed on the bacterial surface. Domain D3 contains a disulfide bond indicated with an "S-S". (B) Western blot probed with a rabbit anti-$Int280_{EPEC}$ polyclonal serum (recognizing domains D1, D2, and D3) of whole-cell protein extracts from EPEC bacteria grown in LB in the presence (+) or absence (−) of 10 mM 2-ME. Intact bacteria, harvested from this culture, were incubated with (+) or without (−) PK. The whole-cell extracts were prepared in urea-SDS sample buffer and boiled (+) or not (−) as indicated. The mobility of unfolded (U) and folded (F) intimin is labeled on the right, and the masses of protein standards are shown on the left (in kilodaltons). (C) Western blot as in panel B of whole-cell protein extracts from *E. coli* K-12 strain UT5600 carrying pCVD438.

(2, 39). Although ATs have limitations for the translocation of certain folded protein domains (27, 28, 32, 46), current data indicate that both native and some heterologous passengers may partially fold in the periplasm before being translocated across the OM (7, 41, 48, 54, 57).

Thus, an alternative model to self-translocation of ATs has been proposed suggesting that secretion may take place through a protein-conducting channel formed in the OM by BamA (formerly YaeT in *E. coli* and Omp85 in *Neisseria*) (5, 39). BamA is a conserved protein present in the OMs of gram-negative bacteria, mitochondria, and plastids, which is essential for the biogenesis of the OM (56, 59). In *E. coli*, BamA forms a large complex in the OM with several lipoproteins (BamB to BamE; formerly YfiO, YfgL, NlpB, and SmpA), which is referred to as the Bam complex (33). A functional Bam complex is needed for the biogenesis of integral OM proteins (OMPs) such as OmpA, OmpF/C, and LamB, all of them having β-barrels embedded in the OM. The Bam complex recruits these OMPs from the periplasm, likely associated with protein chaperones, and then acts as an assembly site for their insertion in the OM (6, 45).

Several protein chaperones have been identified in the periplasm of *E. coli* and other gram-negative bacteria (6, 36). Some of these factors are specialized in the catalysis of distinct protein folding steps, such as disulfide bond formation and isomerization (e.g., DsbA and DsbC) (23) or peptidyl-prolyl *cis*/*trans* isomerization (e.g., FkpA, PpiA, and PpiD) (30), whereas others appear to have a general chaperone activity (e.g., SurA, Skp, and DegP) implicated in the transport of OMPs in the periplasm or preventing their aggregation (34, 49, 58). Independently of their general chaperone function, SurA and DegP have dual activities as peptidyl-prolyl *cis*/*trans* isomerase and protease, respectively (4, 50). Interestingly, the general chaperones SurA, Skp, and DegP appear to have a certain degree of redundancy in their function since all of them have been shown to interact with OMPs in the periplasm, and bacterial strains carrying single null mutations in these genes are still capable of assembling OMPs, albeit at reduced levels. The synthetic lethality associated with the *surA degP* and *surA skp* double mutant strains suggested that SurA and Skp/DegP form two parallel pathways for the transport of OMPs, and at least one of them should be functional for bacterial viability (42). In contrast, the *skp degP* double mutant only exhibited synthetic lethality in specific *E. coli* strains grown at temperatures of 37°C or higher (42, 47).

Recent work with ATs (e.g., IcsA from *Shigella flexneri*) has demonstrated that their periplasmic folding and OM insertion depend on the presence of specific periplasmic chaperones and BamA (25, 41, 57). However, there is no information regarding the folding state of intimin in the periplasm, prior to its translocation across the OM, or about its interaction with periplasmic chaperones or the Bam complex. Accordingly, we sought to investigate the role of periplasmic disulfide bond enzymes (e.g., DsbA), general chaperones (i.e., SurA, Skp, and DegP), and the Bam complex for the secretion of intimin. Using full-length and truncated intimin polypeptides, we demonstrate that periplasmic DsbA catalyzes the formation of the disulfide bond in the D3 domain of intimin and that SurA chaperone and BamA assist the insertion of the N region in the OM. We show that Skp and DegP perform a secondary role for intimin insertion in the OM, although the protease activity of DegP actively participates in the degradation of misfolded intimin.

TABLE 1. *E. coli* strains and plasmids

Strain or plasmid	Genotype and relevant properties[a]	Source or reference
Strains		
EPEC (E2348/69)	EPEC O127:H6/enteropathogenic *E. coli*	20
EHEC (EDL933stx)	EHEC O157:H7 Δ(*stx1 stx2*)/enterohemorrhagic *E. coli* devoid of Shiga-like toxins	20
UT5600	K-12 (F^- λ^-) Δ(*ompT-fepC*)*266*	53
UT5601	UT5600 Δ*araC*	This study
UT*dsbA*	UT5600 *dsbA*::*kan*	54
UT*degP*	UT5601 *degP*::*kan*	This study
UT*skp*	UT5600 *skp*::*kan*	This study
UT*surA*	UT5600 *surA*::*kan*	This study
UTP_{BAD}::*bamA*	UT5601 Zeo^r *araC* P_{BAD}::*bamA*	This study
UT*degP*-P_{BAD}::*bamA*	UT5601 *degP*::*kan* Zeo^r *araC* P_{BAD}::*bamA*	This study
UT*degP*-P_{BAD}::*surA*	UT5601 *degP*::*kan* Zeo^r *araC* P_{BAD}::*surA*	This study
Plasmids		
pAK-Not	*lacI*^{q}-P_{lac} promoter pBR322 ori; Cm^r	53
pCVD438	$Intimin_{EPEC}$ (*eae*), pACYC-ori; Cm^r	15
pInt550	$Intimin_{EHEC}$ fragment 1-550 (E-tag, His) cloned in pAK-Not; Cm^r	This study
pNeae	$Intimin_{EHEC}$ fragment 1-659 (E-tag, His) cloned in pAK-Not; Cm^r	This study
pBAD30	*araC* P_{BAD} promoter, pACYC-ori; Ap^r	21
pBAD-SurA	SurA *E. coli* K-12 cloned in pBAD30; Ap^r	This study

[a] Cm^r, chloramphenicol resistance; Ap^r, ampicillin resistance; Zeo^r, zeocin resistance.

MATERIALS AND METHODS

Bacterial strains and growth conditions. *E. coli* strains used in the experiments described in the present study are listed in Table 1. For induction of full-length or intimin fragments in *E. coli* K-12 strains, bacteria were grown at 37°C (unless indicated otherwise) in Luria-Bertani (LB) medium with shaking (at 160 rpm). Where indicated, growth media were supplemented with D-glucose (0.4 or 2% [wt/vol]), D-arabinose (0.4% [wt/vol]), 10 mM 2-mercaptoethanol (2-ME), 0.05 mM IPTG (isopropyl-β-D-thiogalactopyranoside), and appropriate antibiotics. Antibiotics were used at the following concentrations: chloramphenicol, 30 μg/ml; kanamycin, 50 μg/ml; and zeocin, 40 μg/ml. Zeocin-resistant transformants were selected in LB agar medium with a low salt concentration (NaCl, 5 g/liter). *E. coli* XL1-Blue and DH10B-T1 strains (Stratagene) were used for cloning and plasmid preparation. For analysis of endogenous intimin expression in EPEC, overnight cultures of E2348/69 strain were grown statically in LB medium at 37°C for 16 h, diluted in fresh medium to a final optical density at 600 nm (OD_{600}) of 0.05, and grown under identical conditions for additional 4 h before bacteria were harvested.

The null mutant *E. coli* strains described here were obtained by one-step inactivation of chromosomal genes (11). The conditional mutant *E. coli* strains, in which the natural promoter of *bamA* or *surA* was replaced by the *araC* P_{BAD} promoter, were obtained by λred-driven homologous recombination after transformation with a PCR product containing the zeoRExBAD cassette (a gift from Jean Marc Gigho) (44) and flanking DNA of the *bamA* or *surA* promoter regions. The procedure and materials used for the construction of these mutant strains are detailed in the supplemental material.

Plasmids, DNA constructs, and oligonucleotides. The plasmids used in the present study are summarized in Table 1, and the details of plasmid constructions are described in the supplemental material. All DNA constructs were sequenced (Secugen). The oligonucleotides were synthesized by Sigma Genosys. All of the PCRs were performed with *Vent* DNA polymerase (New England Biolabs).

Protein extract preparation, SDS-PAGE, and Western blots. Whole-cell protein extracts were prepared by mixing 100 μl of a bacterial suspension (OD_{600} of 3.0 in phosphate-buffered saline [PBS]) with the same volume of sodium dodecyl sulfate (SDS) sample buffer (2×) or urea-SDS sample buffer (2×), as indicated. The SDS sample buffer (1×) contains 60 mM Tris-HCl (pH 6.8), 1% (wt/vol) SDS, 5% (vol/vol) glycerol, 0.005% (wt/vol) bromophenol blue, and 1% (vol/vol) 2-ME. The urea-SDS sample buffer (1×) contains 60 mM Tris-HCl (pH 6.8), 2% (wt/vol) SDS, 4 M urea, 5 mM EDTA, 5% (vol/vol) glycerol, 0.005% (wt/vol) bromophenol blue, and 1% (vol/vol) 2-ME. SDS-polyacrylamide gel electrophoresis (PAGE) was performed by using the Miniprotean III electrophoresis system (Bio-Rad). For immunoblotting, the proteins were separated by SDS-PAGE and transferred to a polyvinylidene difluoride membrane (Immobilon-P; Millipore) by using a semidry electrophoresis transfer apparatus (Bio-Rad). For immunodetection of the E-tagged proteins, blots were incubated for 1 h at room temperature with an anti-E-tag monoclonal antibody (MAb)-peroxidase (POD) conjugate (1:2,000; GE Bioscience). GroEL was detected with anti-GroEL MAb-POD conjugate (1:5,000; Sigma). OmpA was detected with specific rabbit polyclonal serum (1:5,000; a gift from Hiroshi Nikaido). Full-length intimin was detected by using a rabbit polyclonal anti-intimin-280_{EPEC} antibody (1:200; a gift from Gad Frankel). Skp, DegP, SurA, and BamA were detected with the specific rabbit polyclonal sera anti-Skp (1:1,000; a gift from Matthias Mueller), anti-MBP-DegP (1:5,000; a gift from Michael Ehrmann), anti-SurA (1:10,000; a gift from Roberto Kolter), and anti-BamA (1:5,000; a gift from Thomas Silhavy). Bound rabbit antibodies were detected with protein A-POD conjugate (1:5,000; Zymed). Membranes were blocked, washed, and developed as previously described (29).

Thiol alkylation assays. To determine the oxidation state of intimin in vivo, an alkylation assay of free thiol groups was performed with the high-molecular-weight PEGylation reagent mPEG-maleimide (mPEG-MAL, 5,000 Da; Nektar Therapeutics). The thiol alkylation protocol described previously (29) was modified for mPEG-MAL. Briefly, bacteria were harvested by centrifugation (3,300 × *g*, 3 min), resuspended to an OD_{600} of 1.0, washed twice with 1 ml of PBS, resuspended in 0.5 ml of buffer AK (80 mM Tris-HCl [pH 6.8], 150 mM NaCl), and divided into four aliquots of 100 μl. Two of them were incubated with 100 mM dithiothreitol (DTT) on ice for 10 min and then incubated at 60°C for an additional 10 min (DTT-treated samples). DTT-treated and untreated samples were washed with PBS twice, and one sample from each group was resuspended in AK buffer containing 10 mM mPEG-MAL, whereas the other two were resuspended in AK buffer. Alkylation reaction was performed by 30 min of incubation at room temperature. The samples were then precipitated with trichloroacetic acid (10% [wt/vol]) for 1 h at 4°C, and the precipitated proteins were recovered by centrifugation (14,000 × *g*, 15 min). Protein pellets were washed once with 1 ml of ice-cold acetone, followed by centrifugation (14,000 × *g*, 15 min). Finally, the protein pellets were air dried and resuspended in 30 μl of AK buffer containing 1% (wt/vol) SDS and 5% (vol/vol) glycerol. Samples were mixed with the same volume of nonreducing urea-SDS-sample buffer (2×) (without 2-ME) before being loaded onto SDS-PAGE gels.

Protease accessibility assays. Bacteria were harvested by centrifugation, washed with PBS, and resuspended to an OD_{600} of 3.0 in PBS. An aliquot of 100 μl from this bacterial suspension was incubated with proteinase K (PK; 40 μg/ml; Roche) for 20 min at 37°C. Subsequently, the serine-protease inhibitor phenylmethylsulfonyl fluoride was added to a 1 mM final concentration to stop proteolysis. The cell suspension was centrifuged (14,000 × *g*, 1 min), and the cell pellet was resuspended in 35 μl of PBS. A total cell extract was made by the addition of the same volume of urea-SDS sample buffer (2×). Finally, the sample was boiled for 30 min, sonicated briefly (5 s; Labsonic B Braun), and centrifuged (14,000 × *g*, 5 min) to remove insoluble material before being loaded onto SDS-PAGE gels.

Flow cytometric analysis. *E. coli* cells (equivalent to a final OD_{600} of 1.0) were harvested from the indicated cultures, washed with PBS (filter sterilized), and resuspended in 1 ml of PBS containing 5% (vol/vol) goat serum. After a 30-min incubation at room temperature, an anti-E-tag MAb (10 μg/ml; Phadia) or a rabbit polyclonal anti-$Int280_{EPEC}$ (1:200)—as indicated—were added to the cell suspension. After 60 min of additional incubation, bacteria were washed three times with 1 ml of PBS and resuspended in 0.5 ml of PBS–5% goat serum containing either Alexa 488-conjugated goat anti-mouse immunoglobulin G (IgG) (1:1,000; Molecular Probes) or Alexa 488-conjugated goat anti-rabbit IgG (1:1,000; Molecular Probes). After an additional incubation for 30 min at room temperature in the dark, the cells were washed twice with PBS and resuspended in 1 ml of PBS for flow cytometer analysis. For each experiment, at least 10,000 cells were analyzed in a cytometer (Coulter EPICS XL-MCL; Beckman Coulter) using 488 nm as the excitation wavelength.

RESULTS

Intimin is highly resistant to denaturation and protease digestion. To validate *E. coli* K-12 as a suitable host for the analysis of intimin secretion, the expression level and stability of intimin was compared in EPEC (strain E2348/69) and *E. coli* K-12 (strain UT5600) harboring plasmid pCVD438 (Table 1). This plasmid carries the *eaeA* gene from EPEC under the control of its natural promoter and was previously used for complementation of Δ*eae* mutants of EPEC and *C. rodentium* (18). EPEC (E2348/69) and *E. coli* K-12 (UT5600/pCVD438) bacteria were grown in LB medium at 37°C to early stationary phase, harvested, and lysed in a SDS-urea sample buffer (2% SDS, 4 M urea). An aliquot of the resulting protein extracts was either boiled or kept at 4°C and subsequently analyzed by Western blotting developed with a rabbit anti-$Int280_{EPEC}$ polyclonal serum (raised against the secreted domains D1, D2, and D3). Protein bands corresponding to intimin were observed with similar intensities in EPEC (Fig. 1B) and *E. coli* UT5600/pCVD438 (Fig. 1C). The intimin bands had a mobility of ~95 kDa in the boiled samples, corresponding to the expected mass of full-length intimin and indicating that the polypeptide was completely denatured after boiling in the SDS-urea buffer (Fig. 1B and C, lane 2). As expected for a folded β-barrel protein, in those samples kept at 4°C intimin showed a faster migration in SDS-PAGE (Fig. 1B and C, lane 1). This heat-modifiable mobility in SDS-PAGE is typical of OMPs and is indicative of their folding as β-barrels, which acquire a compact SDS-resistant structure that migrates faster than the unfolded polypeptide in the electrophoresis (when oligomerization of the folded OMP does not occur). We found that intimin requires boiling in the presence of 4 M urea and 2% SDS for complete unfolding (see the supplemental material), indicating the formation of a very stable β-barrel in both EPEC and *E. coli* K-12.

Intimin also showed high resistance to extracellularly added proteases in EPEC and *E. coli* UT5600/pCVD438. Full-length intimin bands did not exhibit any sign of proteolytic digestion after incubation of intact bacteria with PK (Fig. 1B and C, lane 3) or trypsin (data not shown). Nonetheless, intimin was sensitive to PK digestion when the reducing agent 2-ME was added to the growth medium of EPEC and *E. coli* UT5600/pCVD438. Bacteria grown with 2-ME and incubated with PK showed almost the complete digestion of the full-length intimin band and the simultaneous appearance of an ~66-kDa proteolytic product (Fig. 1B and C, lane 6). The growth of EPEC and *E. coli* UT5600/pCVD438 bacteria with 2-ME did not affect folding of the β-barrel of intimin, as proven by its resistance to urea-SDS denaturation and its heat-modifiable mobility (Fig. 1B and C, lanes 4 and 5), suggesting that the increased sensitivity to PK was caused by alterations elsewhere in the protein (i.e., likely the reduction of a disulfide bond in its secreted C domain; see below). Therefore, these results demonstrate that intimin shows similar expression and stability properties in EPEC and *E. coli* K-12 (UT5600/pCVD438) bacteria, validating *E. coli* K-12 as a host for studying the secretion of intimin.

Periplasmic DsbA catalyzes disulfide-bond formation in intimin. $Intimin_{EPEC}$ contains two Cys residues in its primary sequence (Cys-860 and Cys-937) forming an intra-domain disulfide bond in D3 (3, 35). These Cys residues are conserved in $Intimin_{EHEC}$. It has been shown that mutation Cys-937 to Ala abolishes intimin-dependent actin-rich pedestal formation and colonic hyperplasia (18, 24). To test whether periplasmic DsbA catalyzes the formation of this disulfide bond during the periplasmic transit of intimin, its expression was analyzed in a *dsbA* mutant *E. coli* UT5600*dsbA*/pCVD438 and its isogenic wild-type strain. Flow cytometry analysis of bacteria stained with anti-$Int280_{EPEC}$ indicated that intimin was displayed on the surfaces of wild-type and *dsbA* mutant bacteria (Fig. 2A). The mean fluorescence intensity of *dsbA* mutant bacteria was slightly reduced (~ 30% lower than that of the wild-type strain). A similar reduction was observed in wild-type *E. coli* UT5600/pCVD438 bacteria grown in the presence of 2-ME (Fig. 2A), suggesting a lower stability of secreted intimin in the presence of 2-ME or in the absence of DsbA. Intimin showed identical heat-modifiable mobility and resistance to urea-SDS denaturation in wild-type and *dsbA* mutant bacteria (Fig. 2B). However, as observed under reducing growth conditions (Fig. 1B and C), intimin produced in *dsbA* mutant bacteria was sensitive to PK digestion (Fig. 2B). Therefore, the absence of DsbA does not affect the folding of the β-barrel of intimin but makes intimin less stable and susceptible to protease digestion, likely due to the misfolding of the secreted D3 domain that contains the single disulfide bond between Cys-860 and Cys-937.

To gain a direct evidence of the formation of this disulfide bond by DsbA, the redox state of intimin was compared in wild-type and *dsbA* mutant *E. coli* K-12 strains carrying pCVD438. For this purpose, an alkylation assay was performed with the polyethylene glycol (PEG)-conjugated maleimide mPEG-MAL (5,000 Da) that covalently binds to free sulfydryl groups in proteins. Binding of mPEG-MAL can be monitored by determining the shift in the mobility of the protein in nonreducing SDS-PAGE. As a positive control, EPEC bacteria were also subjected to alkylation with mPEG-MAL followed by nonreducing SDS-PAGE. This experiment revealed that intimin reacts to mPEG-MAL when expressed in the *dsbA* mutant, in which a high-molecular-weight band corresponding to alkylated intimin appears (Fig. 2C, lane 7). In contrast, intimin expressed in wild-type EPEC or UT5600/pCVD438 bacteria was not reactive to the alkylating agent (Fig. 2C, lanes 2 and 5) unless the disulfide bond in D3 was reduced by the incubation of bacteria with the reducing agent DTT (Fig. 2C, lane 3). Mock alkylation of an intimin deletion lacking the D1, D2, and D3 domains (named Neae) demonstrated the specificity of the alkylation reaction (see Fig. S1 in the supplemental material). Collectively, these results demonstrate that periplas-

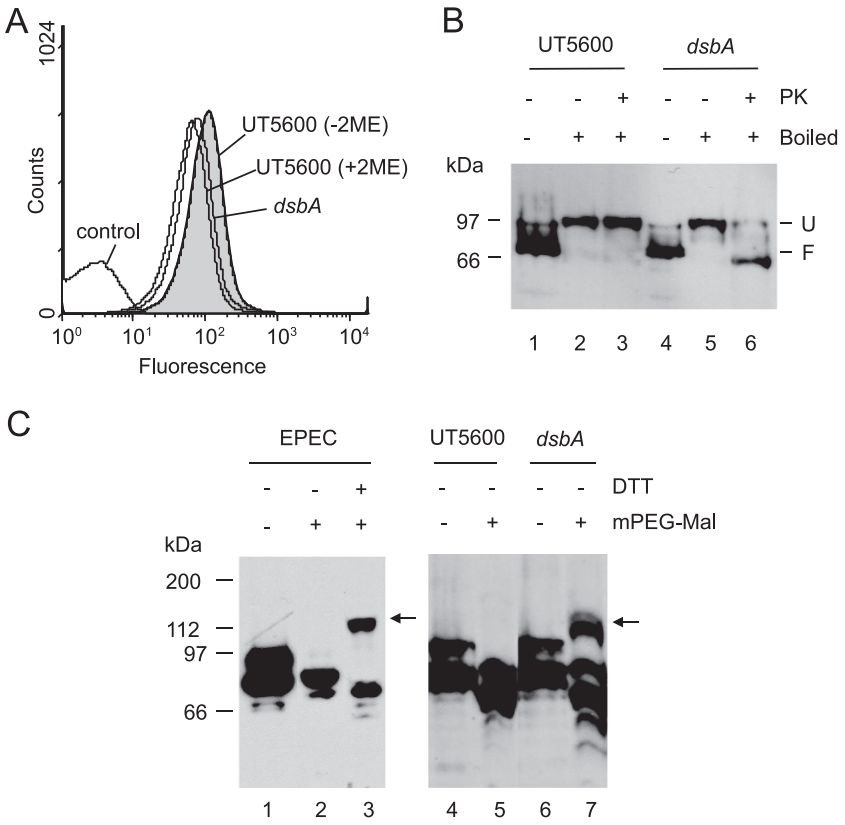

FIG. 2. DsbA-dependent disulfide bond formation in intimin. (A) Flow cytometry analysis to determine the display of intimin on the surface of wild-type *E. coli* UT5600/pCVD438, grown at 30°C in the presence or absence (as indicated) of 10 mM 2-ME, and in its isogenic *dsbA* mutant (harboring pCVD438) grown in the absence of 2-ME. Bacteria carrying the empty vector (pAK-Not) were used as a negative control. Intact bacteria were incubated with rabbit anti-$Int280_{EPEC}$ and Alexa 488-conjugated goat anti-rabbit IgG antibodies. (B) Western blot probed with anti-$Int280_{EPEC}$ serum of whole-cell protein extracts in urea-SDS sample buffer of *E. coli* UT5600 and its isogenic *dsbA* mutant carrying pCVD438. Samples were treated as in Fig. 1. (C) Alkylation with mPEG-MAL of intimin expressed in EPEC, UT5600/pCVD438 and UT*dsbA*/pCVD438, to determine the presence of its disulfide bond in vivo. Treated samples were subjected to nonreducing SDS-PAGE and Western blotting developed with anti-$Int280_{EPEC}$ serum. Samples incubated with the reducing agent DTT and/or with the alkylating agent mPEG-MAL are indicated (+). The bands corresponding to alkylated intimin polypeptide are labeled with arrows. The masses of protein standards are shown on the left (in kilodaltons).

mic DsbA catalyzes the formation of the disulfide bond present in the D3 domain of intimin, suggesting that this domain is at least partially folded in the periplasm prior to its OM translocation.

Expression and folding of intimin in *surA*-, *skp*-, and *degP*-null mutants. To investigate the dependence of intimin on the periplasmic chaperones SurA, Skp, and DegP, individual isogenic null mutants were constructed in *E. coli* UT5600 (Table 1) by deleting the corresponding genes by homologous recombination (see the supplemental material). The phenotype of the isolated single mutant strains was confirmed by the absence of the corresponding periplasmic chaperone in Western blot (see Fig. S2 in the supplemental material). Constitutive expression of full-length intimin (from plasmid pCVD438) in the wild type and in *surA*, *skp*, and *degP* single mutants was analyzed with anti-$Int280_{EPEC}$ by flow cytometry (Fig. 3A) and Western blotting (Fig. 3B) after growth at 37°C. This analysis revealed that intimin was displayed on the surface of the wild type and all mutant strains with the expected heat-modifiable mobility of a folded β-barrel protein. Nevertheless, the levels of intimin in the *surA* mutant strain were considerably reduced. Both, the mean fluorescence intensity in flow cytometry (Fig. 3A) and the intensity of the protein bands in a Western blot (Fig. 3B) indicated a reduction of ~4-fold in the level of intimin in the *surA* mutant. Analysis of the distribution of bacteria in the flow cytometry histograms in three independent experiments indicated that the percentage of *surA* mutant bacteria with a high level of intimin on their surface ($\geq 10^3$ fluorescence units) was ~9%, whereas it represented ~39% in the wild-type strain. In contrast, flow cytometry and Western blot analysis of the expression and surface display of intimin in the *skp* mutant showed on average a modest ~1.5-fold reduction (Fig. 3). In addition, no differences in surface display or intimin expression were observed in the *degP* mutant (Fig. 3). Thus, these data suggest that intimin has a higher dependency on SurA than on Skp/DegP to reach a high level of display on the surface of *E. coli*.

To specifically address the role of SurA, Skp, and DegP chaperones in the insertion of intimin in the OM, the expression and folding of a truncated intimin devoid of the secreted D0, D1, D2, and D3 domains was analyzed. This polypeptide comprises the first 550 amino acids of intimin (named Int550),

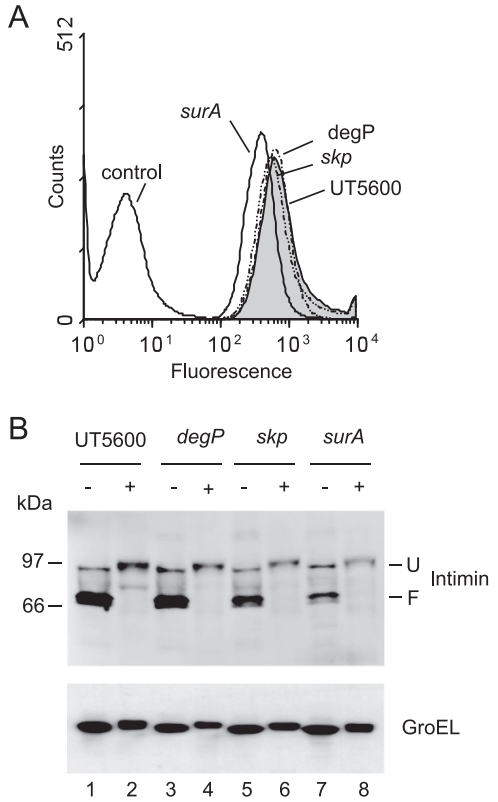

FIG. 3. Expression and folding of intimin in *E. coli* mutants lacking DegP, Skp, or SurA. (A) Flow cytometry analysis to determine the presence of intimin on the surface of wild-type *E. coli* (UT5600) or in its isogenic *degP*, *skp*, and *surA* mutants transformed with pCVD438. The antibodies used and the negative control were as described in Fig. 2. (B) Western blot probed with anti-Int280$_{EPEC}$ serum (upper panel) of whole-cell protein extracts prepared in urea-SDS sample buffer of wild-type UT5600 and *degP*, *skp*, and *sur*A isogenic mutants carrying pCVD438. Detection of GroEL (lower panel) with anti-GroEL MAb-POD was used as a loading control. The mobility of unfolded (U) and folded (F) forms of intimin are indicated. The masses of protein standards are shown on the left (in kilodaltons).

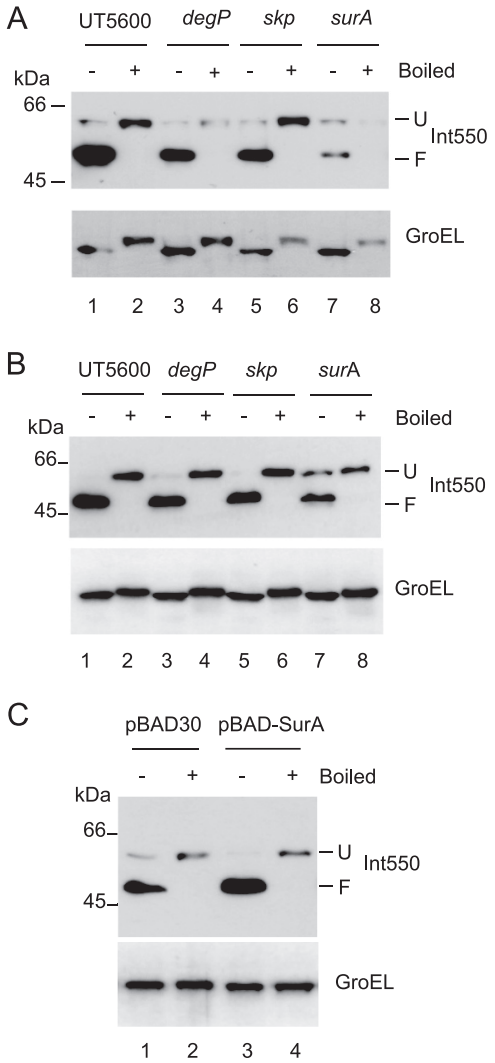

FIG. 4. Expression and folding of Int550 deletion construct in *E. coli degP*-, *skp*-, and *surA*-null mutants. (A) Western blot of wild-type (UT5600) bacteria or *degP*, *skp*, and *surA* isogenic mutants carrying pInt550 and grown at 37°C in LB medium containing IPTG. (B) Western blot of bacteria as in panel A but grown in LB at 30°C and induced at mid-exponential phase with IPTG for 3 h. (C) Western blot of UT*surA*-null mutant strain carrying pInt550 and one of the indicated plasmids, pBAD30 (negative control) or pBAD-SurA (for complementation of the *surA* mutation), grown at 30°C in LB with L-arabinose and induced at mid-exponential phase with IPTG for 3 h. In all cases (A, B, and C) whole-cell protein extracts were prepared in urea-SDS sample buffer, boiled or not as indicated ("+" or "–", respectively), and probed with anti-E-tag MAb-POD for detection of Int550 (upper panels) or with anti-GroEL MAb-POD to dectect GroEL as a loading control. The mobility of unfolded (U) and folded (F) forms of Int550 is labeled. The masses of protein standards are shown on the left of each blot (in kilodaltons).

and it inserts in the OM, forming a homodimer (52). Int550 is 98% identical in EPEC (E2348/69) and EHEC (EDL933) strains. In our construct (pInt550) two short epitopes (the E-tag [GAPVPYPDLEPA] and the His_6 tag) were fused at the C terminus of Int550 for immune detection. The Int550 construct was validated by its capacity to transport the above-mentioned epitopes to the bacterial surface (see Fig. S3A in the supplemental material), by its heat-modifiable electrophoretic mobility and resistance to urea-SDS (see Fig. S3B in the supplemental material), and by its localization in the OM fraction as a dimer according to Blue-Native PAGE (see Fig. S3C in the supplemental material). When Int550 expression was induced in *E. coli* by the continuous presence of IPTG throughout bacterial growth at 37°C (equivalent to the conditions used for the constitutive expression of the full-length intimin from pCVD348), a strong reduction of Int550 (>5-fold) was observed in the *surA*-null mutant strain (Fig. 4A, compare lanes 1 and 7), and a significant fraction of Int550 was found in its unfolded conformation (Fig. 4A, lane 7). In contrast, in the *degP*- or *skp*-null mutants only a moderate twofold reduction in the level of Int550 was observed, and the fraction of unfolded polypeptide remained similar to that detected in the wild-type strain (Fig. 4A, compare lanes 1, 3, and 5). The heat-modifiable mobility of Int550 was confirmed by boiling an aliquot of these samples (lanes 2, 4, 6, and 8). We found that detection of Int550 by MAb anti-E-tag is frequently lower in the boiled aliquots than in the unboiled samples (compare the

signal intensity in lanes 1, 3, 5, and 7 to that in lanes 2, 4, 6, and 8). This difference in signal intensity between boiled and unboiled samples was not always reproducible, and the reason for this is unclear for us, but it likely reflects some modification of the E-tag epitope after boiling in SDS-urea buffer.

To confirm the accumulation of unfolded Int550 in the *surA* mutant, the expression of Int550 was analyzed in bacteria grown at 30°C to minimize protease activities (e.g., DegP) and induced with IPTG for only 3 h when cultures reached OD_{600} ~0.5. Under these growth and induction conditions the *degP* and *skp* mutants did not show any significant decrease in the level of Int550 compared to the wild-type strain (Fig. 4B). On the contrary, the level of folded Int550 was significantly reduced (>3-fold) in the *surA* mutant, and an accumulation of unfolded Int550 was clearly observed (Fig. 4B, compare lanes 1 and 7). Complementation of the *surA* mutant with a plasmid expressing SurA under the control of P_{BAD} promoter (pBAD-SurA; see Fig. S4 in the supplemental material), but not with the empty vector pBAD30, restores wild-type levels of Int550 and eliminates the accumulation of unfolded Int550 under similar experimental conditions (i.e., cultures grown at 30°C with L-arabinose and induced by IPTG for 3 h) (Fig. 4C). Taken together, these results indicate that in the absence of SurA the Skp/DegP pathway is not sufficient to fold and insert high levels of intimin or Int550 in the OM, suggesting that SurA is the main periplasmic chaperone that participates in the secretion of intimin.

Folding of Int550 in a *degP surA* depletion strain. Previous studies with *surA*-null mutants have shown that the constitutive absence of this chaperone leads to the induction of the σ^E-dependent extracytoplasmic stress response (4, 43) and of small RNAs inhibiting the synthesis of several OMPs (55). Induction of σ^E- and Cpx-envelope stress responses leads to an upregulation of Skp and DegP levels (10), which is observed in the *surA* mutant strain used in the present study (see Fig. S2 in the supplemental material). To confirm that the effects in intimin observed in the *surA* mutant were directly dependent on the absence of SurA and not due to a general stress response, we assessed the expression and folding of Int550 upon SurA depletion to avoid a full induction of envelope stress responses. For this purpose, we constructed a conditional double mutant *degP surA* depletion strain, named UT*degP*-P_{BAD}::*surA* (see the supplemental material), in which *degP* is disrupted by a kanamycin resistance cassette and the inducible *araC*-P_{BAD} promoter cassette replaces the native promoter of *surA* on the chromosome (Table 1). The transcriptional activity of the P_{BAD}::*surA* allele can be controlled by the presence in the growth medium of the inducer L-arabinose or of the repressor D-glucose. Under repression conditions, SurA is depleted from the cell. The simultaneous absence of DegP in this strain blocks the alternative Skp/DegP pathway for OMP transport and allows the accumulation of misfolded OMPs in the periplasm. A similar approach was performed to define the role of periplasmic chaperones in the biogenesis of integral OMPs (49).

The simultaneous absence of the SurA and Skp/DegP pathways is reported to inhibit the growth of *E. coli* (42, 49). To test this phenotype, the UT*degP*-P_{BAD}::*surA* strain was grown overnight in the presence of L-arabinose and then subcultured in medium containing either 0.4% L-arabinose or 0.4% D-glucose. Repeated dilutions in the respective media were carried out to maintain bacteria in the exponential growth phase. As shown in the growth curve of Fig. 5A, UT*degP*-P_{BAD}::*surA* bacteria grow normally in the nondepletion medium, but their growth stopped in the depletion medium after the second dilution. The isogenic wild-type and *degP* strains grew normally in the presence of L-arabinose or D-glucose (data not shown). These data confirmed the synthetic lethal phenotype of UT*degP*-P_{BAD}::*surA* caused by the absence of SurA and Skp/DegP pathways under repression conditions.

Int550 was produced in UT*degP*-P_{BAD}::*surA* bacteria grown in repressing medium (D-glucose) at 37°C, and its folding was analyzed at different time points corresponding to the dilutions of the culture (indicated by roman numerals in Fig. 5). Whole-cell extracts in standard SDS buffer (to avoid any unfolding of Int550 during sample preparation) were analyzed by Western blotting under nondenaturing (nonboiling) conditions with specific antibodies to detect: Int550, OmpA (an internal positive control), SurA (to monitor its depletion), Skp (to monitor induction of envelope stress responses), and GroEL (as internal loading control). As shown in Fig. 5B, an accumulation of the unfolded Int550 polypeptide is observed in the samples corresponding to the time points in which SurA is depleted (II and III; lanes 4 and 5, respectively). A similar result was obtained for OmpA in this strain (Fig. 5B), as expected from its reported dependence on SurA (43). Controls for folded and unfolded Int550 and OmpA bands were included (lanes 1 and 2). Importantly, Skp levels were not upregulated during the experiment compared to the Skp levels found at the preinoculum when SurA is present (Fig. 5B), ruling out a full induction of envelope stress responses. Taken together, these results indicate that depletion of SurA causes the accumulation of unfolded Int550 and confirms a direct involvement of SurA chaperone in the folding of the β-barrel domain of intimin.

BamA is required for the insertion of Int550 in the OM. Depletion of BamA from *E. coli* cells leads to an impaired OM biogenesis and a reduction in the levels of integral OMPs such as OmpF/C, OmpA, and TolC (6, 45). To investigate whether the Bam complex is responsible for the OM insertion of the β-barrel domain of intimin, the expression and folding of Int550 was analyzed in a *bamA* conditional depletion strain because the *bamA*-null mutation is lethal in *E. coli* (59). Using an approach similar to that used for the *surA* depletion strain, the native promoter of *bamA* was replaced by the inducible *araC*-P_{BAD} promoter in the chromosome of *E. coli*, generating the strain UTP_{BAD}::*bamA*. In addition, to test whether DegP is also involved in the proteolytic processing of Int550 in a BamA depletion background, a double-mutant strain UT*degP*-P_{BAD}::*bamA* was constructed (see the supplemental material).

Growth of strain UTP_{BAD}::*bamA* (Fig. 6A) at 37°C under glucose repression resulted in growth retardation after the second dilution (II) of the exponentially growing culture and led to a total growth arrest after the third dilution (III). Growth of the *degP bamA* depletion strain showed a similar growth arrest under glucose repression (Fig. 6B). Nevertheless, this double mutant exhibited growth retardation even before the second dilution (Fig. 6B), suggesting a more severe phenotype of the depletion of BamA in the absence of DegP.

Folding of Int550 was assessed in UTP_{BAD}::*bamA* and

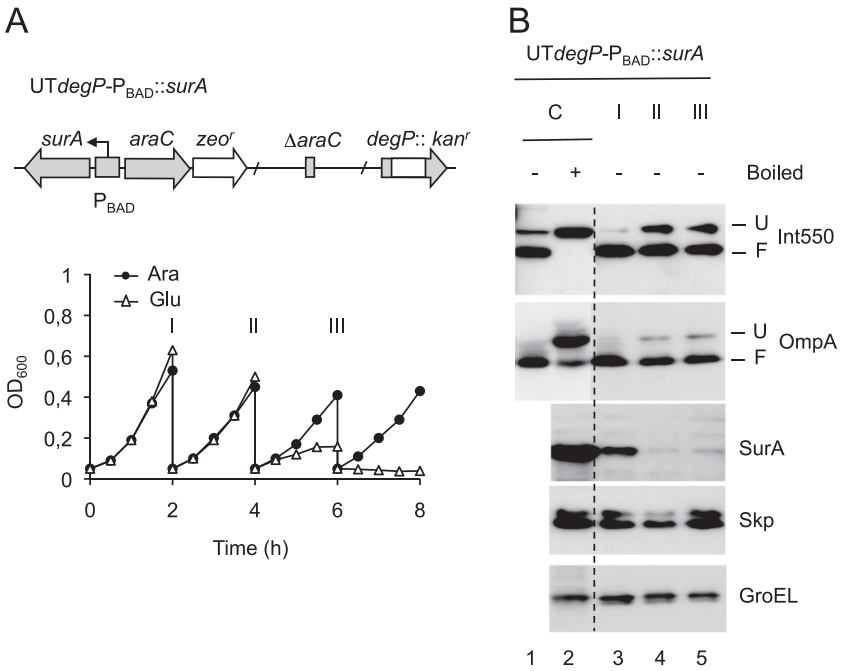

FIG. 5. Folding of Int550 in a *degP surA* depletion mutant. (A) Growth curve of the *E. coli* UT*degP*-P_{BAD}::*surA* strain in the presence of arabinose (●) or glucose (△). The Roman numerals (I, II, and III) indicate the time points at which the bacterial cultures were diluted to maintain exponential growth. A scheme of the chromosomal *surA* and *degP* alleles in this strain is shown on top. (B) Aliquots of a culture of *E. coli* UT*degP*-P_{BAD}::*surA*/pInt550 grown with glucose to deplete SurA were taken at various time points prior to culture dilution (indicated with Roman numerals as in panel A). Whole-cell protein extracts were prepared in standard SDS buffer, subjected to Western blotting, and probed with anti-E-tag MAb-POD, anti-OmpA, anti-SurA, anti-Skp, or anti-GroEL-POD serum. Unfolded (U) and folded (F) forms of Int550 and OmpA are labeled. Control bands (C, lanes 1 and 2) of unfolded and folded Int550 and OmpA were obtained from whole-cell protein extracts prepared from the overnight culture grown in the presence of arabinose and used as the inoculum for the experiment (lanes 1 and 2). Control protein extracts were prepared in urea-SDS buffer (Int550) or in standard SDS buffer (OmpA) and boiled or not as indicated ("+" or "–", respectively).

UT*degP*-P_{BAD}::*bamA* and isogenic wild-type cells (UT5601) growing under glucose-repression at 37°C. Bacteria were harvested at the indicated time points (I, II, and III), lysed in standard SDS sample buffer under nonboiling conditions, and subjected to Western blotting to detect Int550, OmpA (as a positive control), BamA (to monitor its depletion), and GroEL (an internal loading control) (Fig. 6C). Controls for folded and unfolded Int550 and OmpA bands were included (lanes 1 and 2). This assay revealed that the levels of Int550 and OmpA were reduced dramatically when BamA is depleted in UTP_{BAD}::*bamA* strain (compare lanes 3 to 5 and lanes 6 to 8). Importantly, although the levels of Int550 and OmpA decreased in this strain, there was not significant accumulation of the unfolded polypeptides. In contrast, in the UT*degP*-P_{BAD}::*bamA* strain there was a clear accumulation of the unfolded forms of Int550 and OmpA, indicating that DegP is involved in the degradation of periplasmic Int550 (and OmpA) that is not properly inserted in the OM upon BamA depletion. In this double-mutant strain the reduction of folded Int550 and OmpA is less severe than in the UTP_{BAD}::*bamA* strain, likely because in the absence of DegP Int550 and OmpA (and their precursors) may have a longer in vivo half-life.

DISCUSSION

In this study we unveiled the role of periplasmic chaperones and of BamA (formerly YaeT/Omp85) in the folding and OM insertion of intimin. The periplasmic chaperones selected are involved either in specific steps of protein folding (e.g., DsbA, disulfide bond formation) (37) or participate in two alternative pathways for the transport of OMPs in the periplasm of *E. coli* (SurA and Skp/DegP pathways) (36, 49). The role of BamA was investigated since this conserved OMP is an essential component of a large protein complex required for assembly of integral β-barrel OMPs in *E. coli* (6, 59).

First, we found that DsbA was required for the correct folding of the secreted C-region of intimin. DsbA was needed for the formation of a disulfide bond present in the lectin D3 domain of intimin. In the absence of DsbA, the C region of intimin was translocated to the cell surface but was sensitive to PK, indicating that it is misfolded. Since DsbA catalyzes disulfide bond formation in the periplasm, this result implies that, in the wild-type strain, the D3 domain of intimin contains a tertiary structure prior to its translocation to the extracellular milieu. Therefore, the hydrophilic pore used for translocation of the secreted domains of intimin across the OM should have the capacity to accommodate a folded (or at least partially folded) D3 domain. The diameter of the folded D3 lectin domain, and that of the secreted immunoglobulinlike D0, D1, and D2 domains is ~2.0 nm (3, 35). In contrast to these observations with the natural C domain of intimin, previous work with heterologous proteins containing disulfide bonds (e.g., β-lactamase and BLIP) fused to intimin fragment 1-659 at its C terminus revealed that these heterologous polypeptides

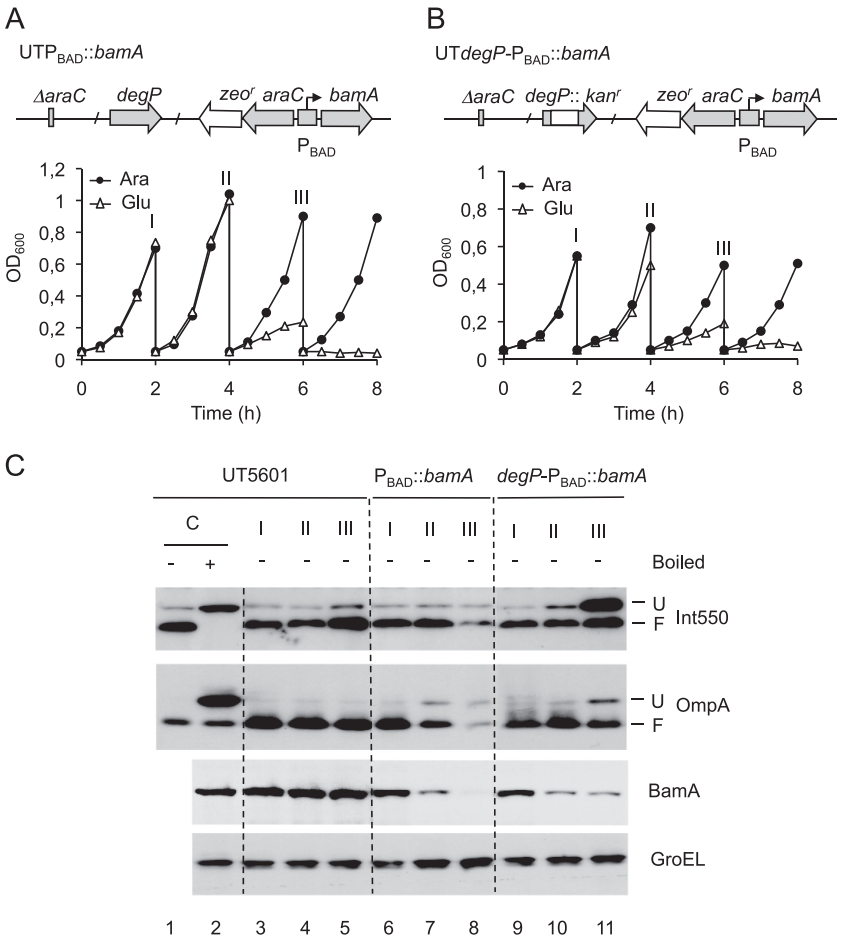

FIG. 6. Folding of Int550 in *bamA* depletion strains. (A and B) Growth curves of the *E. coli* UTP$_{BAD}$::*bamA* (A) and UT*degP*-P$_{BAD}$::*bamA* (B) strains in the presence of arabinose (●) or glucose (△). The Roman numerals (I, II, and III) indicate the time points at which the bacterial cultures were diluted to maintain exponential growth. Schemes of the chromosomal *bamA* and *degP* alleles in these strains are shown at the top of each growth curve. (C) Aliquots of cultures of *E. coli* strains UT5601, UTP$_{BAD}$::*bamA*, and UT*degP*-P$_{BAD}$::*bamA* carrying pInt550 (grown with glucose to deplete BamA) were taken at the indicated time points (by Roman numerals). Western blot analysis was done as described in Fig. 5B to detect Int550, OmpA, BamA, and GroEL. Control bands (C, lanes 1 and 2) of unfolded and folded Int550 and OmpA were obtained from protein extracts of *E. coli* UT5601/pInt550 as described in Fig. 5B.

were not translocated to the bacterial surface (1). Similar controversy can be found with ATs. Although research with natural passengers of ATs (e.g., IcsA and EspP) have shown that some degree of protein folding is acquired in the periplasm (7, 27, 41, 48), work with disulfide-bond containing heterologous proteins, such as cholera toxin B or β-lactamase, fused as N passengers indicated that formation of disulfide-bond blocked OM translocation. Interestingly, when immunoglobulin domains containing disulfide bonds have been used as heterologous AT passengers for the IgA protease (from *Neisseria gonorrhoeae*), OM translocation was not blocked (54). Therefore, intimin and ATs appear to have a similar tolerance for the translocation of immunoglobulin domains with disulfide bonds across the OM, although other protein domains with disulfide bonds block secretion.

The data presented here demonstrate that intimin employs the periplasmic SurA chaperone as the major periplasmic pathway for its secretion. The Skp/DegP pathway can be used for intimin transport, but to a much lesser extent. Strains deficient in Skp or DegP only showed a marginal effect on the expression or surface display level of intimin. On the contrary, in a *surA* null mutant, in which the Skp/DegP pathway is functional and its components upregulated, the level of intimin is reduced fourfold compared to the wild-type strain. The absence of SurA also results in low display levels of intimin, as demonstrated by flow cytometry. The fraction of bacteria expressing a high level of intimin on their surface is especially low in the absence of SurA.

A reduced level of the N-terminal fragment of intimin Int550, which contains the β-barrel of intimin, was also observed in the absence of SurA. Interestingly, the unfolded form of Int550 accumulates in the *surA* mutant, further demonstrating the importance of a functional SurA pathway for the efficient insertion of intimin in the OM. In addition, when Int550 is expressed in a *degP surA* double-mutant depletion strain (grown under nonpermissive conditions in which both pathways are inactive), the unfolded form of Int550 rapidly accumulated in the bacterium. Curiously, we did not observe an accumulation of unfolded full-length intimin in the *surA*-null mutant, perhaps because the presence of the D0, D1, D2, and

D3 domains make this polypeptide more susceptible to proteolytic degradation by DegP in the periplasm. Collectively, this information indicates that intimin is mainly selecting the SurA pathway versus the Skp/DegP pathway for its secretion and that the protease activity of DegP is responsible for the degradation of the unfolded polypeptide that is not inserted in the OM. Our data are in agreement with recent data suggesting a major role of the SurA pathway for the assembly of integral OMPs in *E. coli* (49). Nevertheless, simultaneous use of the SurA and Skp/DegP pathways has been suggested for the assembly of OMPs in *E. coli* (42), as well as for some ATs (e.g., IcsA from *S. flexneri*) (41, 57). Therefore, although intimin selects preferentially the SurA pathway for secretion, other members of the type V secretion system (e.g., IcsA) may require both the SurA and the Skp/DegP pathways for high levels of display. Selection of the different pathways may depend on factors such as the secreted protein itself and the environmental conditions (e.g., temperature). Importantly, DegP has a higher chaperone activity at low temperatures (34, 50).

Our work also shows that the insertion of intimin in the OM depends on BamA. When BamA is depleted from bacteria, Int550 is not assembled in the OM, and the unfolded form accumulates in the bacterium when DegP is absent. These data demonstrate the essential role of BamA for the insertion of intimin in the OM and a role of the protease activity of DegP in the degradation of intimin in the periplasm. The Bam complex has been shown to be essential for the biogenesis of β-barrels proteins such as integral OMPs (e.g., OmpA, LamB, OmpF/C, PhoE and TolC) (6, 45) and ATs (e.g., IcsA) (25). Interestingly, the Bam complex is not needed for the OM insertion of a special group of OMPs that seems to have a distinct structure (i.e., based on amphipathic α-helices) (9, 14). Therefore, the requirement of BamA for the insertion of intimin is likely due to the presence of a β-barrel in its N region. It has been proposed that the Bam complex might be needed not only for the insertion of the β-barrel domain of ATs in the OM but also for the translocation of the passenger domains (5, 39). The Bam-dependent translocation model is attractive because it could explain how ATs are able to translocate some folded protein domains (e.g., immunoglobulin domains of ~2.0 nm), but their "transport" domains (a β-barrel with an α-helix inside) do not have a hydrophilic pore wide enough to accommodate them (2, 39). In this model, the Bam complex would provide the hydrophilic pore for the translocation of these folded protein domains. Interestingly, the presence of hydrophilic pores of variable sizes has been reported in lipid membranes containing BamA (51).

Intimin has obvious structural differences with ATs, including a distinct three-dimensional structure of their secreted domains made by a β-helix rod in ATs (40) versus a rod of immunoglobulinlike domains in intimin. Despite these differences, their need of periplasmic chaperones and BamA for correct folding and OM insertion and their tolerance for the secretion of partially folded domains are common features for both systems. These common aspects strongly suggest that intimin and ATs could use a similar mechanism for the translocation of their secreted domains.

ACKNOWLEDGMENTS

We thank Gad Frankel (Imperial College London), Jean-Marc Ghigo (Institute Pasteur), Hiroshi Nikaido (University of California Berkeley), Michael Ehrmann (University of Duisburg-Essen), Matthias Muller (University of Freiburg), Roberto Kolter (Harvard Medical School), and Natividad Ruiz and Thomas Silhavy (University of Princeton) for kindly providing biological materials used in this study. We thank Sandra Sánchez Poza (University of Santiago de Compostela) for technical advice on Blue-Native PAGE.

This study was supported by grants to L.A.F. from the Spanish Ministry of Science (BIO2005-03964 and BIO2008-05201), the Autonomous Community of Madrid (S-BIO-236-2006), and the VI Framework Program from the European Union (FP6-LSHB-CT-2005-512061 NoE EuroPathogenomics). G.B. was a holder of the postdoctoral contract Juan de la Cierva from the Spanish Ministry of Science. E.M. is a holder of a predoctoral contract of Autonomous Community of Madrid.

We declare no conflict of interest.

REFERENCES

1. **Adams, T. M., A. Wentzel, and H. Kolmar.** 2005. Intimin-mediated export of passenger proteins requires maintenance of a translocation-competent conformation. J. Bacteriol. **187:**522–533.
2. **Barnard, T. J., N. Dautin, P. Lukacik, H. D. Bernstein, and S. K. Buchanan.** 2007. Autotransporter structure reveals intra-barrel cleavage followed by conformational changes. Nat. Struct. Mol. Biol. **14:**1214–1220.
3. **Batchelor, M., S. Prasannan, S. Daniell, S. Reece, I. Connerton, G. Bloomberg, G. Dougan, G. Frankel, and S. Matthews.** 2000. Structural basis for recognition of the translocated intimin receptor (Tir) by intimin from enteropathogenic *Escherichia coli*. EMBO J. **19:**2452–2464.
4. **Behrens, S., R. Maier, H. de Cock, F. X. Schmid, and C. A. Gross.** 2001. The SurA periplasmic PPIase lacking its parvulin domains functions in vivo and has chaperone activity. EMBO J. **20:**285–294.
5. **Bernstein, H. D.** 2007. Are bacterial "autotransporters" really transporters? Trends Microbiol. **15:**441–447.
6. **Bos, M. P., V. Robert, and J. Tommassen.** 2007. Biogenesis of the gram-negative bacterial outer membrane. Annu. Rev. Microbiol. **61:**191–214.
7. **Brandon, L. D., and M. B. Goldberg.** 2001. Periplasmic transit and disulfide bond formation of the autotransported *Shigella* protein IcsA. J. Bacteriol. **183:**951–958.
8. **Buist, G., A. Steen, J. Kok, and O. P. Kuipers.** 2008. LysM, a widely distributed protein motif for binding to (peptido)glycans. Mol. Microbiol. **68:**838–847.
9. **Collin, S., I. Guilvout, M. Chami, and A. P. Pugsley.** 2007. YaeT-independent multimerization and outer membrane association of secretin PulD. Mol. Microbiol. **64:**1350–1357.
10. **Dartigalongue, C., D. Missiakas, and S. Raina.** 2001. Characterization of the *Escherichia coli* sigma E regulon. J. Biol. Chem. **276:**20866–20875.
11. **Datsenko, K. A., and B. L. Wanner.** 2000. One-step inactivation of chromosomal genes in *Escherichia coli* K-12 using PCR products. Proc. Natl. Acad. Sci. USA **97:**6640–6645.
12. **Dautin, N., and H. D. Bernstein.** 2007. Protein secretion in gram-negative bacteria via the autotransporter pathway. Annu. Rev. Microbiol. **61:**89–112.
13. **Deng, W., Y. Li, B. A. Vallance, and B. B. Finlay.** 2001. Locus of enterocyte effacement from *Citrobacter rodentium*: sequence analysis and evidence for horizontal transfer among attaching and effacing pathogens. Infect. Immun. **69:**6323–6335.
14. **Dong, C., K. Beis, J. Nesper, A. L. Brunkan-Lamontagne, B. R. Clarke, C. Whitfield, and J. H. Naismith.** 2006. Wza the translocon for *E. coli* capsular polysaccharides defines a new class of membrane protein. Nature **444:**226–229.
15. **Donnenberg, M. S., and J. B. Kaper.** 1991. Construction of an eae deletion mutant of enteropathogenic *Escherichia coli* by using a positive-selection suicide vector. Infect. Immun. **59:**4310–4317.
16. **Elliott, S. J., L. A. Wainwright, T. K. McDaniel, K. G. Jarvis, Y. K. Deng, L. C. Lai, B. P. McNamara, M. S. Donnenberg, and J. B. Kaper.** 1998. The complete sequence of the locus of enterocyte effacement (LEE) from enteropathogenic *Escherichia coli* E2348/69. Mol. Microbiol. **28:**1–4.
17. **Frankel, G., D. C. Candy, P. Everest, and G. Dougan.** 1994. Characterization of the C-terminal domains of intimin-like proteins of enteropathogenic and enterohemorrhagic *Escherichia coli*, *Citrobacter freundii*, and *Hafnia alvei*. Infect. Immun. **62:**1835–1842.
18. **Frankel, G., A. D. Phillips, M. Novakova, H. Field, D. C. Candy, D. B. Schauer, G. Douce, and G. Dougan.** 1996. Intimin from enteropathogenic *Escherichia coli* restores murine virulence to a *Citrobacter rodentium eaeA* mutant: induction of an immunoglobulin A response to intimin and EspB. Infect. Immun. **64:**5315–5325.
19. **Garmendia, J., G. Frankel, and V. F. Crepin.** 2005. Enteropathogenic and

enterohemorrhagic *Escherichia coli* infections: translocation, translocation, translocation. Infect. Immun. **73:**2573–2585.

20. **Garmendia, J., A. D. Phillips, M. F. Carlier, Y. Chong, S. Schuller, O. Marches, S. Dahan, E. Oswald, R. K. Shaw, S. Knutton, and G. Frankel.** 2004. TccP is an enterohaemorrhagic *Escherichia coli* O157:H7 type III effector protein that couples Tir to the actin-cytoskeleton. Cell Microbiol. **6:**1167–1183.
21. **Guzman, L. M., D. Belin, M. J. Carson, and J. Beckwith.** 1995. Tight regulation, modulation, and high-level expression by vectors containing the arabinose PBAD promoter. J. Bacteriol. **177:**4121–4130.
22. **Hamburger, Z. A., M. S. Brown, R. R. Isberg, and P. J. Bjorkman.** 1999. Crystal structure of invasin: a bacterial integrin-binding protein. Science **286:**291–295.
23. **Heras, B., S. R. Shouldice, M. Totsika, M. J. Scanlon, M. A. Schembri, and J. L. Martin.** 2009. DSB proteins and bacterial pathogenicity. Nat. Rev. Microbiol. **7:**215–225.
24. **Higgins, L. M., G. Frankel, I. Connerton, N. S. Goncalves, G. Dougan, and T. T. MacDonald.** 1999. Role of bacterial intimin in colonic hyperplasia and inflammation. Science **285:**588–591.
25. **Jain, S., and M. B. Goldberg.** 2007. Requirement for YaeT in the outer membrane assembly of autotransporter proteins. J. Bacteriol. **189:**5393–5398.
26. **Jerse, A. E., and J. B. Kaper.** 1991. The *eae* gene of enteropathogenic *Escherichia coli* encodes a 94-kilodalton membrane protein, the expression of which is influenced by the EAF plasmid. Infect. Immun. **59:**4302–4309.
27. **Jong, W. S. P., C. M. ten Hagen-Jongman, T. den Blaauwen, D. Jan Slotboom, J. R. H. Tame, D. Wickstrom, J.-W. de Gier, B. R. Otto, and J. Luirink.** 2007. Limited tolerance toward folded elements during secretion of the autotransporter Hbp. Mol. Microbiol. **63:**1524–1536.
28. **Jose, J., J. Krämer, T. Klauser, J. Pohlner, and T. F. Meyer.** 1996. Absence of periplasmic DsbA oxidoreductase facilitates export of cysteine-containing passenger proteins to the *Escherichia coli* cell surface via the Igaβ autotransporter pathway. Gene **178:**107–110.
29. **Jurado, P., D. Ritz, J. Beckwith, V. de Lorenzo, and L. A. Fernández.** 2002. Production of functional single-chain Fv antibodies in the cytoplasm of *Escherichia coli*. J. Mol. Biol. **320:**1–10.
30. **Justice, S. S., D. A. Hunstad, J. R. Harper, A. R. Duguay, J. S. Pinkner, J. Bann, C. Frieden, T. J. Silhavy, and S. J. Hultgren.** 2005. Periplasmic peptidyl prolyl *cis-trans* isomerases are not essential for viability, but SurA is required for pilus biogenesis in *Escherichia coli*. J. Bacteriol. **187:**7680–7686.
31. **Kaper, J. B., J. P. Nataro, and H. L. Mobley.** 2004. Pathogenic *Escherichia coli*. Nat. Rev. Microbiol. **2:**123–139.
32. **Klauser, T., J. Pohlner, and T. F. Meyer.** 1990. Extracellular transport of cholera toxin B subunit using *Neisseria* IgA protease β-domain: conformation-dependent outer membrane translocation. EMBO J. **9:**1991–1999.
33. **Knowles, T. J., A. Scott-Tucker, M. Overduin, and I. R. Henderson.** 2009. Membrane protein architects: the role of the BAM complex in outer membrane protein assembly. Nat. Rev. Microbiol. **7:**206–214.
34. **Krojer, T., J. Sawa, E. Schafer, H. R. Saibil, M. Ehrmann, and T. Clausen.** 2008. Structural basis for the regulated protease and chaperone function of DegP. Nature **453:**885–890.
35. **Luo, Y., E. A. Frey, R. A. Pfuetzner, A. L. Creagh, D. G. Knoechel, C. A. Haynes, B. B. Finlay, and N. C. Strynadka.** 2000. Crystal structure of enteropathogenic *Escherichia coli* intimin-receptor complex. Nature **405:**1073–1077.
36. **Mogensen, J. E., and D. E. Otzen.** 2005. Interactions between folding factors and bacterial outer membrane proteins. Mol. Microbiol. **57:**326–346.
37. **Nakamoto, H., and J. C. Bardwell.** 2004. Catalysis of disulfide bond formation and isomerization in the *Escherichia coli* periplasm. Biochim. Biophys. Acta **1694:**111–119.
38. **Newman, C. L., and C. Stathopoulos.** 2004. Autotransporter and two-partner secretion: delivery of large-size virulence factors by gram-negative bacterial pathogens. Crit. Rev. Microbiol. **30:**275–286.
39. **Oomen, C. J., P. Van Ulsen, P. Van Gelder, M. Feijen, J. Tommassen, and P. Gros.** 2004. Structure of the translocator domain of a bacterial autotransporter. EMBO J. **23:**1257–1266.
40. **Otto, B. R., R. Sijbrandi, J. Luirink, B. Oudega, J. G. Heddle, K. Mizutani, S.-Y. Park, and J. R. H. Tame.** 2005. Crystal structure of hemoglobin protease, a heme binding autotransporter protein from pathogenic *Escherichia coli*. J. Biol. Chem. **280:**17339–17345.
41. **Purdy, G. E., C. R. Fisher, and S. M. Payne.** 2007. IcsA surface presentation in *Shigella flexneri* requires the periplasmic chaperones DegP, Skp, and SurA. J. Bacteriol. **189:**5566–5573.
42. **Rizzitello, A. E., J. R. Harper, and T. J. Silhavy.** 2001. Genetic evidence for parallel pathways of chaperone activity in the periplasm of *Escherichia coli*. J. Bacteriol. **183:**6794–6800.
43. **Rouvière, P. E., and C. A. Gross.** 1996. SurA, a periplasmic protein with peptidyl-prolyl isomerase activity, participates in the assembly of outer membrane porins. Genes Dev. **10:**3170–3182.
44. **Roux, A., C. Beloin, and J. M. Ghigo.** 2005. Combined inactivation and expression strategy to study gene function under physiological conditions: application to identification of new *Escherichia coli* adhesins. J. Bacteriol. **187:**1001–1013.
45. **Ruiz, N., D. Kahne, and T. J. Silhavy.** 2006. Advances in understanding bacterial outer-membrane biogenesis. Nat. Rev. Microbiol. **4:**57–66.
46. **Rutherford, N., M. E. Charbonneau, F. Berthiaume, J. M. Betton, and M. Mourez.** 2006. The periplasmic folding of a cysteineless autotransporter passenger domain interferes with its outer membrane translocation. J. Bacteriol. **188:**4111–4116.
47. **Schäfer, U., K. Beck, and M. Muller.** 1999. Skp, a molecular chaperone of gram-negative bacteria, is required for the formation of soluble periplasmic intermediates of outer membrane proteins. J. Biol. Chem. **274:**24567–24574.
48. **Skillman, K. M., T. J. Barnard, J. H. Peterson, R. Ghirlando, and H. D. Bernstein.** 2005. Efficient secretion of a folded protein domain by a monomeric bacterial autotransporter. Mol. Microbiol. **58:**945–958.
49. **Sklar, J. G., T. Wu, D. Kahne, and T. J. Silhavy.** 2007. Defining the roles of the periplasmic chaperones SurA, Skp, and DegP in *Escherichia coli*. Genes Dev. **21:**2473–2484.
50. **Spiess, C., A. Beil, and M. Ehrmann.** 1999. A temperature-dependent switch from chaperone to protease in a widely conserved heat shock protein. Cell **97:**339–347.
51. **Stegmeier, J. F., and C. Andersen.** 2006. Characterization of pores formed by YaeT (Omp85) from *Escherichia coli*. J. Biochem. **140:**275–283.
52. **Touze, T., R. D. Hayward, J. Eswaran, J. M. Leong, and V. Koronakis.** 2004. Self-association of EPEC intimin mediated by the b-barrel-containing anchor domain: a role in clustering of the Tir receptor. Mol. Microbiol. **51:**73–87.
53. **Veiga, E., V. de Lorenzo, and L. A. Fernández.** 1999. Probing secretion and translocation of a beta-autotransporter using a reporter single-chain Fv as a cognate passenger domain. Mol. Microbiol. **33:**1232–1243.
54. **Veiga, E., V. De Lorenzo, and L. A. Fernández.** 2004. Structural tolerance of bacterial autotransporters for folded passenger protein domains. Mol. Microbiol. **52:**1069–1080.
55. **Vogel, J., and K. Papenfort.** 2006. Small non-coding RNAs and the bacterial outer membrane. Curr. Opin. Microbiol. **9:**605–611.
56. **Voulhoux, R., M. P. Bos, J. Geurtsen, M. Mols, and J. Tommassen.** 2003. Role of a highly conserved bacterial protein in outer membrane protein assembly. Science **299:**262–265.
57. **Wagner, J. K., J. E. Heindl, A. N. Gray, S. Jain, and M. B. Goldberg.** 2009. Contribution of the periplasmic chaperone Skp to efficient presentation of the autotransporter IcsA on the surface of *Shigella flexneri*. J. Bacteriol. **191:**815–821.
58. **Walton, T. A., C. M. Sandoval, C. A. Fowler, A. Pardi, and M. C. Sousa.** 2009. The cavity-chaperone Skp protects its substrate from aggregation but allows independent folding of substrate domains. Proc. Natl. Acad. Sci. USA **106:**1772–1777.
59. **Wu, T., J. Malinverni, N. Ruiz, S. Kim, T. J. Silhavy, and D. Kahne.** 2005. Identification of a multicomponent complex required for outer membrane biogenesis in *Escherichia coli*. Cell **121:**235–245.